Three-Dimensional Finite-Element Method with Edge Elements for Electromagnetic Waveguide Discontinuities

Kiyoshi Ise, Kazuhiro Inoue, and Masanori Koshiba, *Senior Member, IEEE*

Abstract —**When three-dimensional electromagnetic problems are solved by the finite-element method based on a functional with three components of electric or magnetic field, spurious solutions appear if the traditional tetrahedral elements are used. This paper shows that the finite-element method using edge elements succeeds in suppressing spurious solutions and moreover that this method succeeds in the analysis of three-dimensional electromagnetic waveguide problems with metal wedges.**

I. Introduction

In general, the finite-element analysis of three-dimensional electromagnetic problems is based on a functional with three components of electric or magnetic field. However, when the eigenvalue problems are solved with this functional, it is found that spurious solutions not satisfying the condition $\nabla \cdot \boldsymbol{H} = 0$ appear if traditional tetrahedral elements are used [1], [2].

Recently it has been reported that spurious solutions appear in three-dimensional electromagnetic discontinuity problems and that the penalty function method is effective in suppressing these spurious solutions, but a new kind of spurious solution, one dependent on the penalty coefficient, is generated [3]. The penalty function method is the one that makes the condition $\nabla \cdot \boldsymbol{H} = 0$ be satisfied in a least-squares manner [4]–[7].

In this paper a method using edge elements is introduced to suppress spurious solutions. This method makes the condition $\nabla \cdot \boldsymbol{H} = 0$ be satisfied in each element. It is confirmed that spurious solutions do not appear when the finite-element method using edge elements is applied to three-dimensional electromagnetic discontinuity problems.

It is noted that the finite-element method using three components cannot adequately treat three-dimensional electromagnetic waveguide problems with metal wedges, because the transverse part of the magnetic or electric field is infinite at a sharp metal edge [8], [9] and the piecewise polynomials traditionally associated with finite elements cannot accurately represent an infinite field.

Manuscript received November 5, 1990; revised March 18, 1991.
The authors are with the Department of Electronic Engineering, Hokkaido University, Sapporo, 060 Japan.
IEEE Log Number 9101025.

Webb succeeds in predicting dispersion in two-dimensional waveguide problems with sharp metal edges by the finite-element method using singular trial functions which model the singular behavior of the field close to sharp edges [9]. However, it may be difficult to develop this method and apply it to the three-dimensional problems.

This paper shows that it is difficult to prescribe boundary conditions on the fine points of metal wedges when the finite-element method using traditional tetrahedral elements is applied to three-dimensional electromagnetic waveguide problems with metal wedges. On the other hand, variables for edge elements are not at vertices but at edges, so that it is unnecessary to prescribe boundary conditions at the fine points of metal wedges. We show that edge elements, therefore, may be available for the analysis of arbitrarily shaped waveguides.

II. Variational Formulation

The waveguide junction as shown in Fig. 1 is considered. The junction may be connected with rectangular waveguides or may be loaded with arbitrarily shaped dielectric. Here the boundary plane Γ_i connects the discontinuity region Ω to the rectangular waveguide i ($i = 1,2$), and the region Ω surrounded by Γ_1, Γ_2, and Γ_0 encloses the waveguide discontinuities completely. Γ_0 is assumed to be a perfectly conducting wall.

From Maxwell's equation, the following vectorial wave equation is derived with respect to the magnetic field $\boldsymbol{H}$:

$$\nabla \times (\epsilon^{-1} \nabla \times \boldsymbol{H}) - k_0^2 \boldsymbol{H} = 0 \tag{1}$$

where

$$k_0^2 = \omega^2 \epsilon_0 \mu_0. \tag{2}$$

The problem defined by (1) may be formulated variationally [10], [11] and the functional $F(\boldsymbol{H})$ is expressed as follows:

$$F(\boldsymbol{H}) = \iiint_\Omega (\nabla \times \boldsymbol{H})^* \cdot (\epsilon^{-1} \nabla \times \boldsymbol{H})\, d\Omega - k_0^2 \iiint_\Omega \boldsymbol{H}^* \cdot \boldsymbol{H} d\Omega + \iint_\Gamma \boldsymbol{H}^* \cdot \boldsymbol{n} \times (\epsilon^{-1} \nabla \times \boldsymbol{H})\, d\Gamma \tag{3}$$

0018-9480/91/0800-1289$01.00 ©1991 IEEE

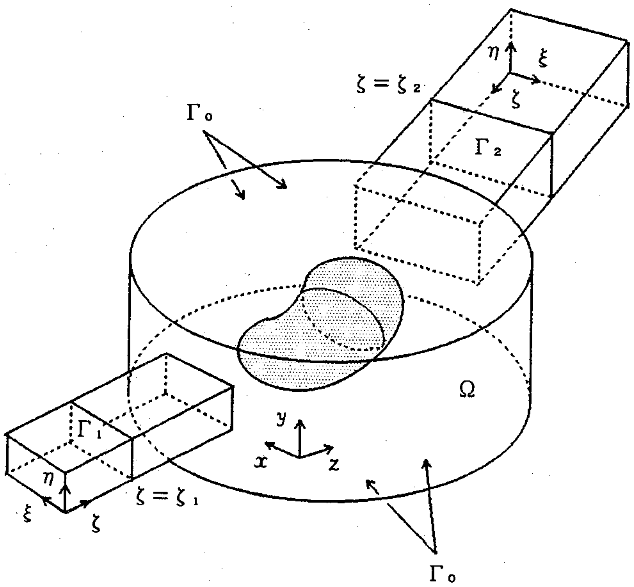

Fig. 1. Waveguide discontinuities.

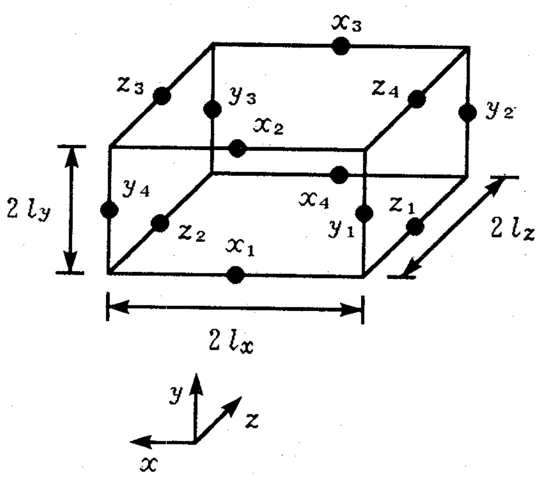

Fig. 2. Edge element.

where $\iiint_\Omega d\Omega$ is the volume integral in the region Ω, $\iint_\Gamma d\Gamma$ is the surface integral over the boundary Γ $(=\Gamma_1+\Gamma_2+\Gamma_0)$, $\boldsymbol{n}$ is the outward unit normal vector on the boundary Γ, and $*$ indicates complex conjugate.

III. Finite-Element Formulation

The region Ω is divided into rectangular parallelepipeds as shown in Fig. 2. The magnetic field H_r $(r=x,y,z)$ in each element is approximated by edge elements [12]–[16]. In the edge element, each edge of a rectangular parallelepiped has a variable which consists of only one component of the magnetic field in the direction of the edge. H_r is expanded in terms of the values of H_r at four nodes in the element as follows:

$$H_r=\{N^r\}^T\{H_r\}_e, \qquad r=x,y,z \tag{4}$$

where $\{H_r\}_e$ is the nodal magnetic field vector in each element, T indicates a transpose, and the shape function vector $\{N^r\}$ is expressed as

$$\{N^x\}=\begin{bmatrix}N_1^x\\N_2^x\\N_3^x\\N_4^x\end{bmatrix}=\begin{bmatrix}1/4[1-(y-y_c)/l_y][1-(z-z_c)/l_z]\\1/4[1+(y-y_c)/l_y][1-(z-z_c)/l_z]\\1/4[1+(y-y_c)/l_y][1+(z-z_c)/l_z]\\1/4[1-(y-y_c)/l_y][1+(z-z_c)/l_z]\end{bmatrix} \tag{5}$$

$$\{N^y\}=\begin{bmatrix}N_1^y\\N_2^y\\N_3^y\\N_4^y\end{bmatrix}=\begin{bmatrix}1/4[1-(z-z_c)/l_z][1-(x-x_c)/l_x]\\1/4[1+(z-z_c)/l_z][1-(x-x_c)/l_x]\\1/4[1+(z-z_c)/l_z][1+(x-x_c)/l_x]\\1/4[1-(z-z_c)/l_z][1+(x-x_c)/l_x]\end{bmatrix} \tag{6}$$

$$\{N^z\}=\begin{bmatrix}N_1^z\\N_2^z\\N_3^z\\N_4^z\end{bmatrix}=\begin{bmatrix}1/4[1-(x-x_c)/l_x][1-(y-y_c)/l_y]\\1/4[1+(x-x_c)/l_x][1-(y-y_c)/l_y]\\1/4[1+(x-x_c)/l_x][1+(y-y_c)/l_y]\\1/4[1-(x-x_c)/l_x][1+(y-y_c)/l_y]\end{bmatrix}. \tag{7}$$

Here the coordinate (x_c, y_c, z_c) is the center of gravity of the rectangular parallelepiped shown in Fig. 2.

When the finite-element method is applied to (3), the following matrix equation is obtained:

$$[S]\{H\}-k_0^2[T]\{H\}+\sum_{e'}\iint_{e'}j\omega\epsilon_0[N](\boldsymbol{n}_1\times\boldsymbol{E})|_{\Gamma_1}d\Gamma+\sum_{e'}\iint_{e'}j\omega\epsilon_0[N](\boldsymbol{n}_2\times\boldsymbol{E})|_{\Gamma_2}d\Gamma=\{0\} \tag{8}$$

$$[S]=\sum_e\iiint_e[B]\epsilon^{-1}[B]^T d\Omega \tag{9}$$

$$[T]=\sum_e\iiint_e[N][N]^T d\Omega. \tag{10}$$

Here $\boldsymbol{n}_1$ and $\boldsymbol{n}_2$ are the outward unit normal vectors on the boundaries Γ_1 and Γ_2, respectively, Σ_e is the summation over all the elements, $\Sigma_{e'}$ is the summation only over the elements related to the boundaries Γ_1 and Γ_2, $\iiint_e d\Omega$

is the volume integral in each edge element, $\iint_e d\Gamma$ is the surface integral on each element in the boundaries Γ_1 and Γ_2, and $\boldsymbol{E}$ is the electric field vector. The matrices $[B]$ and $[N]$ and the vector $\{H\}$ are given by

$$[B]=\begin{bmatrix} \{0\} & \partial\{N^x\}/\partial z & -\partial\{N^x\}/\partial y \\ -\partial\{N^y\}/\partial z & \{0\} & \partial\{N^y\}/\partial x \\ \partial\{N^z\}/\partial y & -\partial\{N^z\}/\partial x & \{0\} \end{bmatrix} \quad (11)$$

$$[N]=\begin{bmatrix} \{N^x\} & \{0\} & \{0\} \\ \{0\} & \{N^y\} & \{0\} \\ \{0\} & \{0\} & \{N^z\} \end{bmatrix} \quad (12)$$

$$\{H\}=\begin{bmatrix} \{H_x\} \\ \{H_y\} \\ \{H_z\} \end{bmatrix} \quad (13)$$

where $\{H_r\}$ $(r=x,y,z)$ is the vector composed of the value of H_r at all nodes in the entire region Ω and $\{0\}$ is a null vector.

Let $\{H\}_1$ and $\{H\}_2$ be the nodal magnetic field vectors related to the nodes on the boundaries Γ_1 and Γ_2, respectively. Also, let $\{H\}_0$ be the nodal magnetic field vector obtained by removing $\{H\}_1$ and $\{H\}_2$ from $\{H\}$. Then, (8) is rewritten as

$$\begin{bmatrix} [R]_{11} & [R]_{10} & [R]_{12} \\ [R]_{01} & [R]_{00} & [R]_{02} \\ [R]_{21} & [R]_{20} & [R]_{22} \end{bmatrix} \begin{bmatrix} \{H\}_1 \\ \{H\}_0 \\ \{H\}_2 \end{bmatrix} = \begin{bmatrix} -\sum_{e'} \iint_{e'} j\omega\epsilon_0 [N](\boldsymbol{n}_1 \times \boldsymbol{E})|_{\Gamma_1} d\Gamma \\ \{0\} \\ -\sum_{e'} \iint_{e'} j\omega\epsilon_0 [N](\boldsymbol{n}_2 \times \boldsymbol{E})|_{\Gamma_2} d\Gamma \end{bmatrix} \quad (14)$$

where $[R]_{11},\cdots,[R]_{22}$ are the submatrices of the following matrix $[R]$:

$$[R]=[S]-k_0^2[T]. \quad (15)$$

Eliminating $\{H\}_0$ from (14), we obtain the following equation:

$$\begin{bmatrix} [P]_{11} & [P]_{12} \\ [P]_{21} & [P]_{22} \end{bmatrix} \begin{bmatrix} \{H\}_1 \\ \{H\}_2 \end{bmatrix} = \begin{bmatrix} -\sum_{e'} \iint_{e'} j\omega\epsilon_0 [N](\boldsymbol{n}_1 \times \boldsymbol{E})|_{\Gamma_1} d\Gamma \\ -\sum_{e'} \iint_{e'} j\omega\epsilon_0 [N](\boldsymbol{n}_2 \times \boldsymbol{E})|_{\Gamma_2} d\Gamma \end{bmatrix} \quad (16)$$

where

$$[P]_{11}=[R]_{11}-[R]_{10}[R]_{00}^{-1}[R]_{01} \quad (17a)$$

$$[P]_{12}=[R]_{12}-[R]_{10}[R]_{00}^{-1}[R]_{02} \quad (17b)$$

$$[P]_{21}=[R]_{21}-[R]_{20}[R]_{00}^{-1}[R]_{01} \quad (17c)$$

$$[P]_{22}=[R]_{22}-[R]_{20}[R]_{00}^{-1}[R]_{02}. \quad (17d)$$

When the division of the region Ω is not sufficient owing to restrictions imposed by computer memory, the substructure method is introduced in the finite-element method [3], [17]. This method is as follows. First, the analysis region Ω is divided into subregions, and the finite-element method is applied to each subregion. Elimination of internal variables is then iterated for these subregions, and finally the dimension of the matrix equation to be solved can be reduced to the number of the nodes on the input and output boundaries, with this dimension being the same as that of (16).

IV. Analytical Formulation

Assuming that the dominant TE_{10} mode is incident from the left of Γ_1 as shown in Fig. 1, we may relate the transverse electric field $\boldsymbol{E}_{ti}$ to the transverse magnetic field $\boldsymbol{H}_{ti}$ on the boundary Γ_i $(i=1,2)$ as follows [3]:

$$\begin{aligned} \boldsymbol{E}_{ti}(\xi,\eta,\zeta_i) &= \delta_{i1} 2a_{i10} e^{-j\beta_{i10}\zeta_i} \boldsymbol{e}_{110}(\xi,\eta) \\ &- \sum_m \sum_n \frac{1}{j\beta_{imn}} \iint_{\Gamma_i} \boldsymbol{h}_{1mn}^*(\xi',\eta') \\ &\cdot j\omega\mu_0 \boldsymbol{H}_{ti}(\xi',\eta')\, d\xi' d\eta' \boldsymbol{e}_{1mn}(\xi,\eta) \\ &- \sum_m \sum_n \frac{j\beta_{imn}}{-k_0^2} \iint_{\Gamma_i} \boldsymbol{h}_{2mn}^*(\xi',\eta') \\ &\cdot j\omega\mu_0 \boldsymbol{H}_{ti}(\xi',\eta')\, d\xi' d\eta' \boldsymbol{e}_{2mn}(\xi,\eta) \end{aligned} \quad (18)$$

where a_{i10} is the amplitude of the incident mode, and the propagation constant β_{imn} is given by

$$\beta_{imn}=\sqrt{k_0^2-(m\pi/a_i)^2-(n\pi/b_i)^2}. \quad (19)$$

The mode functions $\boldsymbol{e}_{lmn}$ and $\boldsymbol{h}_{lmn}$ $(l=1,2)$ are given by [3]. Equation (18) can be discretized as follows:

$$\begin{bmatrix} \{E_\xi\}_i \\ \{E_\eta\}_i \end{bmatrix} = \begin{bmatrix} \{0\} \\ \delta_{i1}\{g\}_i \end{bmatrix} - \begin{bmatrix} [Z_{\xi\xi}]_i & [Z_{\xi\eta}]_i \\ [Z_{\eta\xi}]_i & [Z_{\eta\eta}]_i \end{bmatrix} \begin{bmatrix} j\omega\mu_0\{H_\xi\}_i \\ j\omega\mu_0\{H_\eta\}_i \end{bmatrix} \quad (20)$$

where $[Z_{\xi\xi}]_i,\cdots,[Z_{\eta\eta}]_i$ are the matrices obtained by discretization of (18), and $\{g\}_i$ is given by [3].

Letting $[A]_{11},[A]_{12},\cdots,[A]_{44}$ be the submatrices of $[P]_{11},\cdots,[P]_{22}$ of (16) and combining (16) with (20), the final matrix equation is obtained as follows:

$$\begin{bmatrix} [\bar{A}]_{11} & [\bar{A}]_{12} & [A]_{13} & [A]_{14} \\ [\bar{A}]_{21} & [\bar{A}]_{22} & [A]_{23} & [A]_{24} \\ [A]_{31} & [A]_{32} & [\bar{A}]_{33} & [\bar{A}]_{34} \\ [A]_{41} & [A]_{42} & [\bar{A}]_{43} & [\bar{A}]_{44} \end{bmatrix} \begin{bmatrix} j\omega\mu_0\{H_\xi\}_1 \\ j\omega\mu_0\{H_\eta\}_1 \\ j\omega\mu_0\{H_\xi\}_2 \\ j\omega\mu_0\{H_\eta\}_2 \end{bmatrix} = \begin{bmatrix} [B]_1^\eta\{g\}_1 \\ \{0\} \\ \{0\} \\ \{0\} \end{bmatrix} \tag{21}$$

where

$$[\bar{A}]_{11} = [A]_{11} + [B]_1^\eta [Z_{\eta\xi}]_1 \tag{22a}$$

$$[\bar{A}]_{12} = [A]_{12} + [B]_1^\eta [Z_{\eta\eta}]_1 \tag{22b}$$

$$[\bar{A}]_{21} = [A]_{21} - [B]_1^\xi [Z_{\xi\xi}]_1 \tag{22c}$$

$$[\bar{A}]_{22} = [A]_{22} - [B]_1^\xi [Z_{\xi\eta}]_1 \tag{22d}$$

$$[\bar{A}]_{33} = [A]_{33} + [B]_2^\eta [Z_{\eta\xi}]_2 \tag{22e}$$

$$[\bar{A}]_{34} = [A]_{34} + [B]_2^\eta [Z_{\eta\eta}]_2 \tag{22f}$$

$$[\bar{A}]_{43} = [A]_{43} - [B]_2^\xi [Z_{\xi\xi}]_2 \tag{22g}$$

$$[\bar{A}]_{44} = [A]_{44} - [B]_2^\xi [Z_{\xi\eta}]_2 \tag{22h}$$

$$[B]_i^\xi = \sum_{e'} \iint_{e'} k_0^2 \{N^\eta\}\{N^\xi\}^T \big|_{\Gamma_i} d\Gamma \tag{23a}$$

$$[B]_i^\eta = \sum_{e'} \iint_{e'} k_0^2 \{N^\xi\}\{N^\eta\}^T \big|_{\Gamma_i} d\Gamma. \tag{23b}$$

Here the ξ and η directions on Γ_i $(i = 1,2)$ correspond to ξ and η shown in Fig. 1, respectively. The values of $H_{ti}(\xi, \eta)$ on Γ_i computed from (21) allow determination of the reflection coefficient S_{11} and transmission coefficient S_{21} of the TE_{10} mode as follows:

$$S_{11} = \frac{\iint_{\Gamma_1} \boldsymbol{h}_{110}^*(\xi,\eta) \cdot j\omega\mu_0 \boldsymbol{H}_{t1}(\xi,\eta)\, d\Gamma - j\beta_{110} a_{110} e^{-j\beta_{110}\zeta_1}}{-j\beta_{110} a_{110} e^{j\beta_{110}\zeta_1}} \tag{24}$$

$$S_{21} = \sqrt{\frac{\beta_{210}}{\beta_{110}}}\, \frac{\iint_{\Gamma_2} \boldsymbol{h}_{110}^*(\xi,\eta) \cdot j\omega\mu_0 \boldsymbol{H}_{t2}(\xi,\eta)\, d\Gamma}{-j\beta_{210} a_{110} e^{j\beta_{210}\zeta_2}}. \tag{25}$$

V. Numerical Results

First, a waveguide loaded with dielectric is considered. When the discontinuity problem shown in Fig. 3 is solved by the finite-element method using the functional (3) it is found that spurious solutions appear if the traditional tetrahedral elements are used [3].

Figs. 4 and 5 show the element division with edge elements and the reflection characteristics, respectively. It is found from Fig. 5 that a spurious solution does not appear. The finite-element method using edge elements is more effective for suppression of spurious solutions than the method using the penalty function method, because a new spurious solution dependent on the penalty coefficient is generated when the penalty function method is introduced in the finite-element method [3].

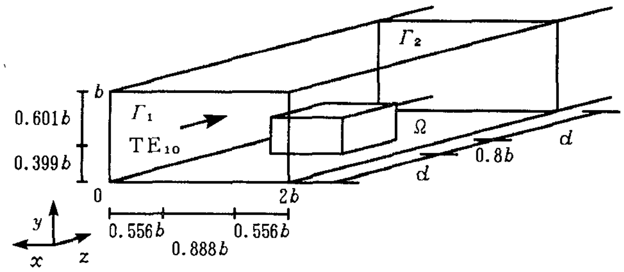

Fig. 3. Dielectric-loaded waveguide. Relative permittivity of dielectric is 6, and the distance d between dielectric edge and Γ_i $(i = 1,2)$ is $0.8b$.

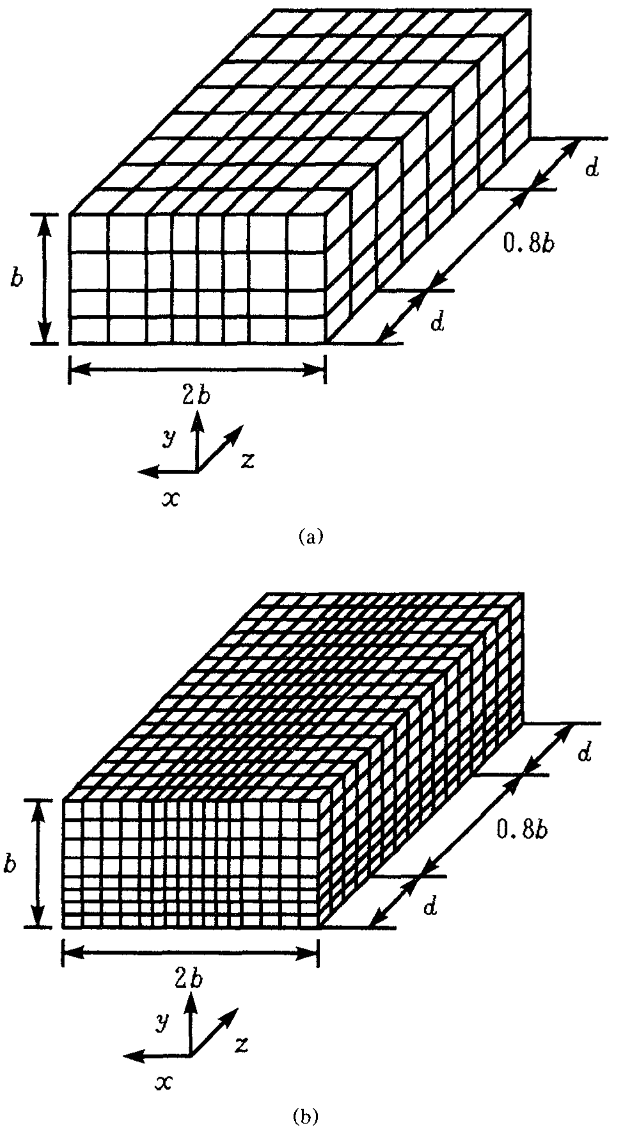

Fig. 4. Element division using edge elements ($d = 0.8b$). (a) Element division #1. (b) Element division #2.

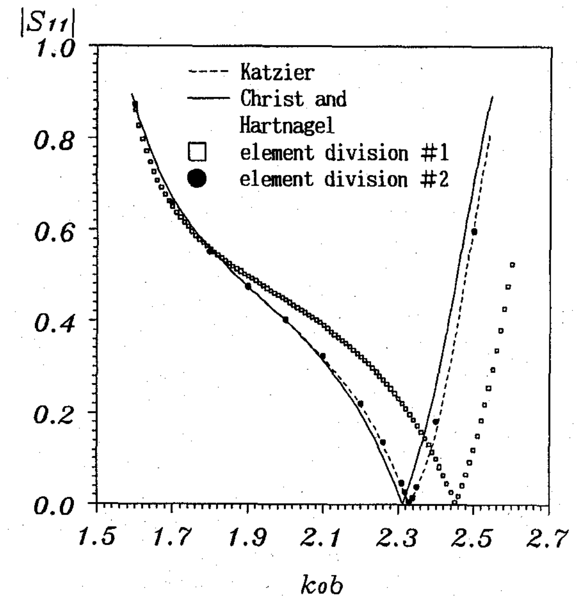

Fig. 5. Reflection characteristics of a dielectric-loaded waveguide.

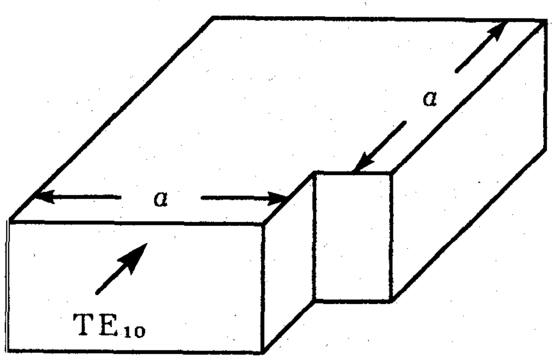

(a)

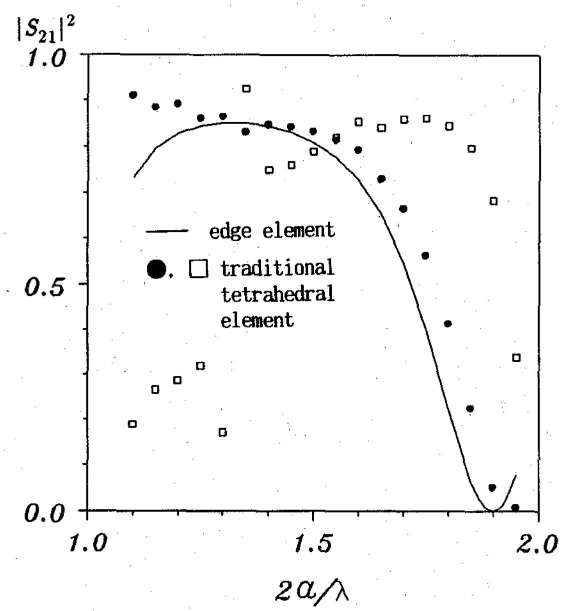

(b)

Fig. 6. Right-angle corner bend. (a) Structure. (b) Power transmission coefficient.

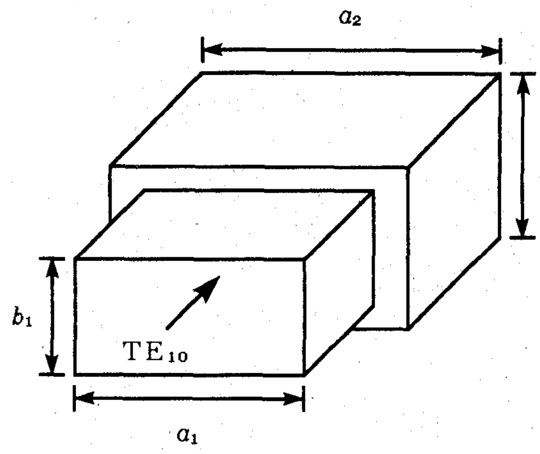

(a)

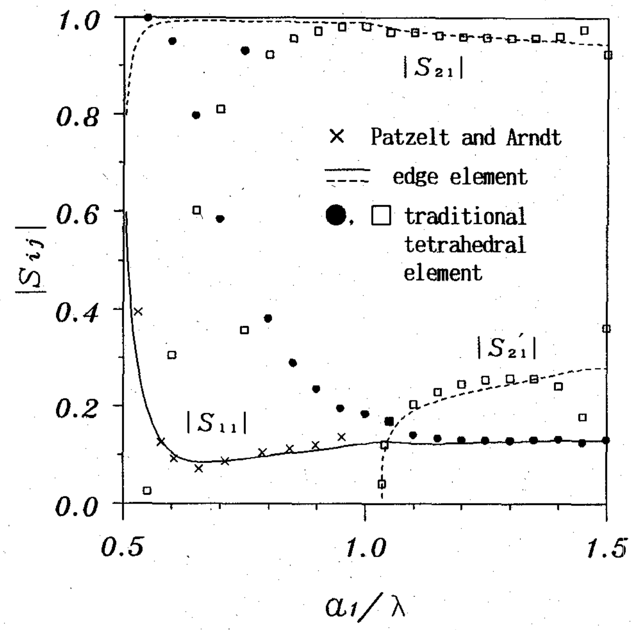

(b)

Fig. 7. Concentric step discontinuity. (a) Structure ($a_1 = 15.8$ mm, $b_1 = 7.9$ mm, $a_2 = 22.9$ mm, $b_2 = 10.2$ mm). (b) Scattering characteristics ($|S'_{21}|$ being the magnitude of the transmission coefficient of the TE_{30} mode).

Reflection coefficients obtained by the element division #1 in Fig. 4(a) disagree with the results of Katzier [18] and of Christ and Hartnagel [19] at higher frequencies. This is because the element division of the region Ω is not sufficient to obtain good numerical convergence. So the substructure method [3] should be introduced to divide the analysis region into many more elements. The results obtained by the element division #2 in Fig. 4(b) for which the substructure method is used agree well with other results [18], [19].

Then, arbitrarily shaped waveguides are considered. When the waveguides with metal wedges shown in Figs. 6(a), 7(a), and 8(a) are analyzed by the finite-element method, it is difficult to prescribe boundary conditions on wedges if the traditional tetrahedral elements are used, because the transverse part of the magnetic or electric field is infinite at fine points of metal wedges [8], [9].

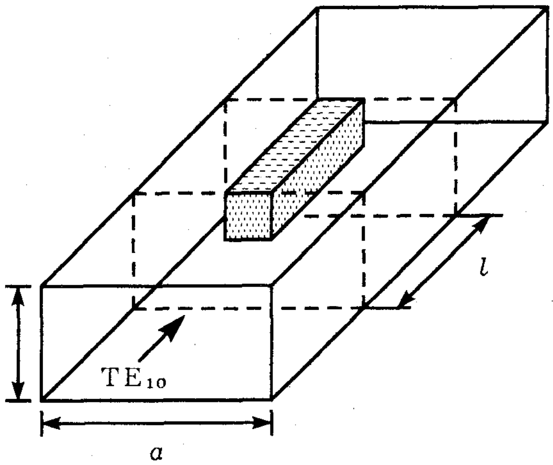

(a)

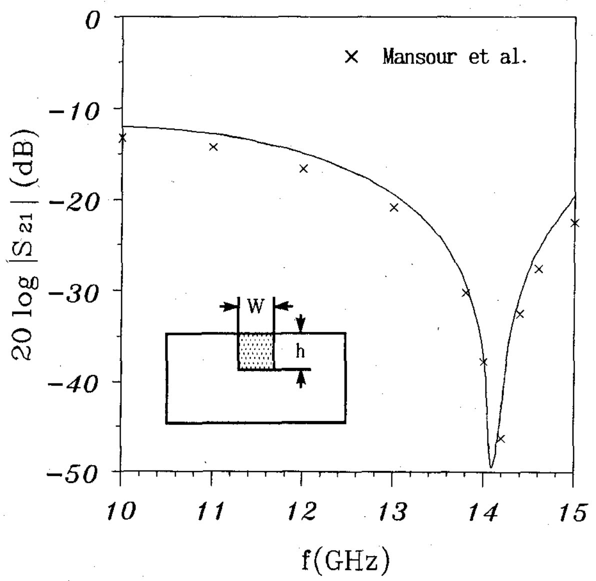

(b)

Fig. 8. *E*-plane ridge waveguide discontinuity. (a) Structure ($a = 19.05$ mm, $b = 9.524$ mm, $l = 5.08$ mm, $W = 1.016$ mm, $h = 7.619$ mm). (b) Transmission characteristics.

Variables for edge elements are not at vertices but at edges, so it is unnecessary to prescribe boundary conditions at fine points of metal wedges. Edge elements therefore may be available for the analysis of arbitrarily shaped waveguides.

Fig. 6(b) shows the transmission characteristics of the waveguide shown in Fig. 6(a). The results of edge elements are shown by the solid line. The results of the penalty function method using tetrahedral elements wherein the field is left free at fine points of a metal wedge and the normal magnetic field there is set to zero are represented by, respectively, dots and squares, with the penalty coefficient s [1]–[3] being 1. The results of the edge elements agree well with those of the two-dimensional finite-element method [20] and boundary-element method [21].

In [22], Picon says that the finite-element method with tetrahedral elements based on three components of the electric field succeeds in solving problems with metal wedges if the condition $\nabla \cdot \boldsymbol{E} = 0$ is imposed on the functional. We also confirm that when the penalty function method is introduced in the finite-element method with tetrahedral elements, a stable field distribution is obtained. But it is clearly seen from Fig. 6(b) that even if the penalty function method is used, correct solutions are not always obtained in the frequency range under consideration.

Fig. 7(b) shows the reflection and transmission characteristics of the concentric step discontinuity shown in Fig. 7(a). The solid and broken lines show the reflection and transmission coefficients obtained by using edge elements, respectively. The dots and squares represent, respectively, the reflection and transmission coefficients obtained by the penalty function method using tetrahedral elements in which the field is left free at fine points of metal wedges and the penalty coefficient s is 1. The results of edge elements agree well with the experimental results, shown by × signs [23]. When the penalty function method with tetrahedral elements is used, incorrect solutions are obtained at certain frequencies in this problem as well.

Fig. 8(b) shows the transmission characteristics of the *E*-plane ridge waveguide discontinuity shown in Fig. 8(a). The results of the edge element, shown by the solid line, agree well with the experimental results, shown by × signs [24].

From the findings described above we expect that the finite-element method using edge elements may be suitable for the analysis of arbitrarily shaped waveguides.

VI. Conclusions

When the finite-element method using edge elements is applied to three-dimensional electromagnetic discontinuity problems, spurious solutions do not appear. Moreover, this method has been successfully applied to three-dimensional problems with metal wedges.

References

[1] M. Koshiba, T. Katano, and M. Suzuki, "Finite-element solution of three-dimensional electromagnetic eigenvalue problems," *Trans. Inst. Electron. Commun. Eng. Japan*, vol. J68-A, pp. 533–540, June 1985 (in Japanese).

[2] K. Inoue, K. Hayata, and M. Koshiba, "Finite-element solution of three-dimensional periodic waveguide problems," *Trans. Inst. Electron. Information Commun. Eng.*, vol. J71-C, pp. 1404–1411, Oct. 1988 (in Japanese).

[3] K. Ise, K. Inoue, and M. Koshiba, "Three-dimensional finite-element solution of dielectric scattering obstacles in a rectangular waveguide," *IEEE Trans. Microwave Theory Tech.*, vol. 38, pp. 1352–1359, Sept. 1990.

[4] M. Koshiba, K. Hayata, and M. Suzuki, "Vectorial finite-element formulation without spurious modes for dielectric waveguides," *Trans. Inst. Electron. Commun. Eng. Japan*, vol. E67, pp. 191–196, Apr. 1984.

[5] B. M. A. Rahman and J. B. Davies, "Penalty function improvement of waveguide solution by finite elements," *IEEE Trans. Microwave Theory Tech.*, vol. MTT-32, pp. 922–928, Aug. 1984.

[6] M. Koshiba, K. Hayata, and M. Suzuki, "Improved finite-element formulation in terms of the magnetic field vector for dielectric

waveguide," *IEEE Trans. Microwave Theory Tech.*, vol. MTT-33, pp. 227–233, Mar. 1985.
[7] J. P. Webb, "The finite-element method for finding modes of dielectric-loaded cavities," *IEEE Trans. Microwave Theory Tech.*, vol. MTT-33, pp. 635–639, July 1985.
[8] R. E. Collin, *Field Theory of Guided Waves*. New York: McGraw-Hill, 1960.
[9] J. P. Webb, "Finite element analysis of dispersion in waveguides with sharp metal edges," *IEEE Trans. Microwave Theory Tech.*, vol. 36, pp. 1819–1824, Dec. 1988.
[10] A. D. Berk, "Variational principles for electromagnetic resonators and waveguides," *IRE Trans. Antennas Propagat.*, vol. AP-4, pp. 104–111, Apr. 1956.
[11] A. Konrad, "Vector variational formulation of electromagnetic fields in anisotropic media," *IEEE Trans. Microwave Theory Tech.*, vol. MTT-24, pp. 553–559, Sept. 1976.
[12] M. Hano, "Finite-element analysis of dielectric-loaded waveguides," *IEEE Trans. Microwave Theory Tech.*, vol. MTT-32, pp. 1275–1279, Oct. 1984.
[13] C. W. Crowley, P. P. Silvester, and H. Hurwitz, "Covariant projection elements for 3D vector field problems," *IEEE Trans. Magn.*, vol. 24, pp. 397–400, Jan. 1988.
[14] A. Bossavit and I. Mayergoyz, "Edge-elements for scattering problems," *IEEE Trans. Magn.*, vol. 25, pp. 2816–2821, July 1989.
[15] A. Kameari, "Calculation of transient 3D eddy current using edge-elements," *IEEE Trans. Magn.*, vol. 26, pp. 466–469, Mar. 1990.
[16] Z. J. Cendes *et al.*, "Integrated microwave field simulation using three-dimensional finite elements," in *IEEE MTT-S Int. Microwave Symp. Dig.* (Dallas), 1990, vol. 2, pp. 721–723.
[17] K. Ise and M. Koshiba, "Dielectric post resonances in a rectangular waveguide," *Proc. Inst. Elec. Eng.*, pt. H, vol. 137, pp. 61–66, Feb. 1990.
[18] H. Katzier, "Streuverhalten elektromagnetischer Wellen bei sprunghaften Übergängen geschirmter dielektrischer Leitungen," *Arch. Elek. Übertragung.*, vol. 38, pp. 290–296, 1984.
[19] A. Christ and H. L. Hartnagel, "Three-dimensional finite-difference method for the analysis of microwave-device embedding," *IEEE Trans. Microwave Theory Tech.*, vol. MTT-35, pp. 688–696, Aug. 1987.
[20] M. Koshiba, M. Sato, and M. Suzuki, "Finite-element analysis of arbitrarily shaped *H*-plane waveguide discontinuities," *Trans. Inst. Electron. Commun. Eng. Japan*, vol. E66, pp. 82–87, Feb. 1983.
[21] M. Koshiba and M. Suzuki, "Application of the boundary-element method to waveguide discontinuities," *IEEE Trans. Microwave Theory Tech.*, vol. MTT-34, pp. 301–307, Feb. 1986.
[22] O. Picon, "Three-dimensional finite-element formulation for deterministic waveguide problems," *Microwave Opt. Technol. Lett.*, vol. 1, pp. 170–172, July 1988.
[23] H. Patzelt and F. Arndt, "Double-plane steps in rectangular waveguides and their application for transformers, irises, and filters," *IEEE Trans. Microwave Theory Tech.*, vol. MTT-30, pp. 771–776, May 1982.
[24] R. Mansour, R. S. K. Tong, and R. H. MacPhie, "Simplified description of the field distribution in finlines and ridge waveguides and its application to the analysis of *E*-plane discontinuities," *IEEE Trans. Microwave Theory Tech.*, vol. 36, pp. 1825–1832, Dec. 1988.

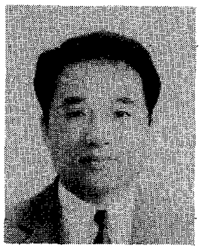

Kiyoshi Ise was born in Kinosaki, Japan, on April 7, 1954. He received the B.S. and M.S. degrees in electronic engineering from Hokkaido University, Sapporo, Japan, in 1986 and 1988, respectively. He is presently studying toward the Ph.D. degree in electronic engineering at Hokkaido University.

Mr. Ise is a member of the Institute of Electronics, Information and Communication Engineers (IEICE).

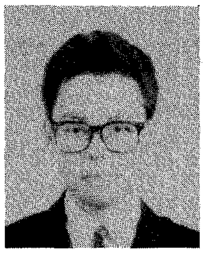

Kazuhiro Inoue was born in Chitose, Hokkaido, Japan, on January 10, 1965. He received the B.S. and M.S. degrees in electronic engineering from Hokkaido University, Sapporo, Japan, in 1987 and 1989, respectively. He is presently studying toward the Ph.D. degree in electronic engineering at Hokkaido University.

Mr. Inoue is a member of the Institute of Electronics, Information and Communication Engineers (IEICE).

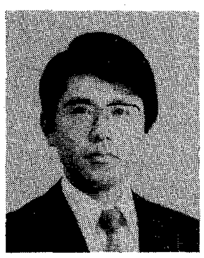

Masanori Koshiba (SM'84) was born in Sapporo, Japan, on November 23, 1948. He received the B.S., M.S., and Ph.D. degrees in electronic engineering from Hokkaido University, Sapporo, Japan, in 1971, 1973, and 1976, respectively.

In 1976, he joined the Department of Electronic Engineering, Kitami Institute of Technology, Kitami, Japan. From 1979 to 1987, he was an Associate Professor of Electronic Engineering at Hokkaido University, and in 1987 he became a Professor there. He has been engaged in research on lightwave technology, surface acoustic waves, magnetostatic waves, microwave field theory, and applications of finite-element and boundary-element methods to field problems.

Dr. Koshiba is a member of the Institute of Electronics, Information and Communication Engineers (IEICE), the Institute of Television Engineers of Japan, the Institute of Electrical Engineers of Japan, the Japan Society for Simulation Technology, and the Japan Society for Computational Methods in Engineering. In 1987, he was awarded the 1986 Paper Award by the IEICE.